Scientific paper

Suitable Chemical Methods for Preparation of Graphene Oxide, Graphene and Surface Functionalized Graphene Nanosheets

Shabnam Sheshmani[1,*] and Marzieh Arab Fashapoyeh[2]

[1] *Department of Chemistry, Shahr-e Rey Branch, Islamic Azad University, P.O. Box 18155-144, Tehran, Iran*

[2] *Department of Chemistry, School of Sciences, Ferdowsi University of Mashhad, Mashhad 917791436, Iran*

** Corresponding author: E-mail: shabnam_sheshmani@iausr.ac.ir*
Tel: +98-21-55229200-9; fax: +98-21-55229297

Received: 26-06-2013

Abstract

This article presents the suitable chemical method for preparation of graphene oxide nanosheets. In order to examine the effects of HNO_3/H_2SO_4 ratio on interlayer spacing and its comparison, the oxidation of graphite with HNO_3 and H_2SO_4 in 1:2 and 1:3 volume ratios was done. Based on the reaction time and interlayer spacing, it was found that the optimum results were obtained when reaction was carried out with HNO_3/H_2SO_4 in 1:3 volume ratio (using modified *Staudenmaier* method) for 4 days. Results showed that the modified *Staudenmaier* method improved efficiency exfoliation in oxidation process. Also, the chemical reduction of graphene oxide, which obtained using the modified *Staudenmaier* method, with hydroquinone and hydrazine hydrate was studied. The results indicate that use of hydrazine hydrate as the reducing agent was more beneficial than the hydroquinone. In continue, we describe the preparation of surface functionalized graphene nanosheets with octadecylamine. The products were characterized by Fourier transform infrared (FT-IR), Raman spectroscopy, X-ray diffraction (XRD), Atomic force microscopy (AFM), Field emission-scanning electron microscopy (FE-SEM) and X-ray photoelectron spectroscopy (XPS).

Keywords: Graphene oxide; Modified *Staudenmaier* method; Graphene; Chemical functionalization; Octadecylamine; Characterization

1. Introduction

A graphite film consisting of only a single atom-thick lattice-shaped layer of carbon is called graphene. Although graphene structure have been known since the 1960s, it was not possible to isolate such a monolayer until a few years ago. The feat was first achieved in 2004 by *Andre Geim* and *Konstantin Novoselov*, who used adhesive tape to peel thin layers off a graphite crystal.[1,2]

Graphene has astounding properties. It is transparent, 100 times stronger than the strongest steel and has a very high electrical and thermal conductivity. These unique properties make graphene an interesting candidate for a number of applications currently under development, as for instance transparent touch screens, light panels or solar cells. Combined with synthetic materials, graphene opens up new vistas for materials that are both highly resistant and very light-weight, to be used, for instance, in satellite or aircraft construction.[3–7] Technological and engineering applications of graphene sheets usually require graphene solutions (or dispersions). Dispersion can be achievable for graphene nanosheets through chemical functionalization, because graphene itself cannot be dispersed in water or in any organic solvent.[8,9]

Graphite powders are usually used as raw materials for bulk production of graphene sheets.[10] Graphite is a 3D network of graphene and is inexpensive. Synthesis of monolayer graphite was tried as early as in 1975, when *B. Lang et al.* showed formation of mono- and multi-layered graphite by thermal decomposition of carbon on single crystal Pt substrates.[11] After a long gap, scattered attempts to produce graphene were reported again from 1999.[12–14] The technique has been and is being followed since then, along with efforts to develop new processing

routes for efficient synthesis of large-scale graphene including micromechanical cleavage and exfoliation,[1] thermal chemical vapor deposition techniques,[15] plasma enhanced chemical vapor deposition techniques,[16,17] chemical methods and other processing routes.[18–22] Among these methods, chemistry approach is the most suitable for producing graphene sheets in large quantity.[23–29] The most common route to chemically exfoliate graphite is the use of strong oxidants to produce graphene oxide. Graphite oxide was first prepared by *B. C. Brodie*, where it was treated with a mixture of $KClO_3$ and nitric acid.[30] Later, *Hummers* and *Offeman* used a mixture of sulfuric acid, sodium nitrate, and potassium permanganate to oxidize graphite.[31] Recently, many papers reporting a modification of the *Hummers* method have been published. For instance, *Marcano et al.* found that used of the $NaNO_3$, increasing the amount of $KMnO_4$, and performing the reaction in a 9:1 mixture of H_2SO_4/H_3PO_4 improves the efficiency of the oxidation process.[32] In *Staudenmaier* method,[33] oxidation of graphite by HNO_3/H_2SO_4 in 1:2 volume ratio in presence of $KClO_3$ in 5 days was carried out.

In this work, the modified *Staudenmaier* method for the preparation of graphene oxide is described. In the literatures, chemical reduction of graphene oxide sheets, which obtained using *Hummers* and *Staudenmaier* methods has been described.[34–36] But, in this article, the effect of two reductant agents (hydroquinone and hydrazine hydrate) and reaction time on reduction of graphene oxide, which obtained based on the modified *Staudenmaier* method has been studied. In addition, the preparation of functionalized graphene nanosheets with octadecylamine was carried out. In earlier reported procedure, initial graphite oxide for preparation of functionalized graphene obtained using the modified *Hummers* method,[37] but in this study graphene oxide prepared *via* the modified *Staudenmaier* method with high exfoliation degree. Fourier transform infrared spectroscopy and Raman spectroscopy indicated the successful preparation of graphene oxide, graphene and functionalized graphene nanosheets. Also, evaluation of these products during the processes was monitored by powder X-ray diffraction. Field emission-scanning electron microscopy and atomic force microscopy were used to demonstrate the morphology and structure of produced graphene oxide, graphene and functionalized graphene nanosheets. Also, in order to identify the types and percentages of the functional groups on the surface of the products, the C1s peaks of the XPS spectra were studied.

2. Experimental

2. 1. Materials and Instruments

Graphite flakes was purchased from Sigma-Aldrich with a particle size of 150 μm and 99.9% purity. Other materials and solvents were of analytical grade, commercially available and used without further purification.

Infrared spectra were recorded as KBr disks on Tensor 27 Bruker spectrophotometer. Raman spectroscopy investigated using a Senterra Bruker with 785 nm diode laser excitation. The evaluation of prepared graphene oxide, graphene and surface functionalized graphene sheets during the processes were monitored by powder X-ray diffraction Philips PW 1800 diffractometer with Cu Ká radiation. Atomic force microscopy was carried out on a Denmark Dualscope/Rasterscope C26, DME microscope. Field emission scanning electron microscopy measurements was performed on a Hitachi S-4160 at an accelerating voltage of 20 kV. The surface chemistry of graphene oxide, graphene and functionalized graphene characterized on X-ray photoelectron spectroscope EA10 plus with Al-Mg anode. The vacuum dried samples was employed to detect the element compositions.

2. 2. Preparation of Graphene Oxide (GO) Nanosheets

Here, *Staudenmaier* and the modified *Staudenmaier* methods were used for preparation of graphene oxide. In the first procedure, graphene oxide was prepared according to the *Staudenmaier* method.[33] Oxidation process was investigated in 1–7 days. In the second route, the modified *Staudenmaier* method was evaluated. In this method, concentrated HNO_3/H_2SO_4 in 1:3 volume ratio was used to prepare graphene oxide. The graphite (1 g) was added under vigorous stirring to cool acid mixture of HNO_3 (63%) and H_2SO_4 (98%) in 1:3 volume ratio. Then, $KClO_3$ (11 g) was added slowly over 2 h to avoid sudden increases in temperature and allowed to stir at room temperature for 4 days. The graphite oxide was re-dispersed in a solution of hydrochloric acid (5% w/w), and washed repeatedly with deionized water until the *p*H of the filtrate was neutral and finally was vacuum dried. The as-obtained graphite oxide was re-dispersed in deionized water and then exfoliated to generate graphene oxide nanosheets by ultrasonication.

2. 3. Preparation of Graphene (G) Nanosheets

The following reduction experiments the initial graphene oxide obtained using the modified *Staudenmaier* method. For the preparation of graphene with hydroquinone as reducing agent, graphite oxide (0.100 g) was dispersed in water (20 mL) through ultrasonication. Then, the hydroquinone (0.125 g) was added to the dispersion. The mixture refluxed at 100 °C for 11 and 22 h. The solid product was isolated by centrifugation, washed with water and ethanol and finally dried. The reduced graphene oxide using hydrazine hydrate as reducing agent was prepared

by the addition of hydrazine hydrate (1 mL) to a dispersion of graphite oxide (0.100 g) in water (100 mL). The mixture was refluxed at 100 °C for 5, 12 and 24 h. The product was isolated by centrifugation, washed with water and methanol and finally dried.

2. 4. Preparation of Functionalized Graphene (G-ODA) Nanosheets

For the preparation of functionalized graphene nanosheets with octadecylamine (ODA), the initial graphite oxide was prepared using the modified *Staudenmaier* method. The similar procedure was reported elsewhere, which graphite oxide was prepared by modified *Hummers* method.[37] In brief, the suspension of graphene oxide (0.200 g) in water (20 mL) was added to octadecylamine (0.200 g) in ethanol (20 mL). The mixture was refluxed at 100 °C for 20 h, once the graphene oxide reacted with octadecylamine to form the GO-ODA. Then, hydroquinone (0.250 g) was added, and the mixture was refluxed for another 22 h to reduce GO-ODA to G-ODA. The solid product was isolated by centrifugation, washed with water and ethanol and finally dried.

3. Results and Discussion

3. 1. Characterization of Graphene Oxide Nanosheets

Mixtures of HNO_3/H_2SO_4 (ratios of 1:2 and 1:3) and $KClO_3$ were oxidized the natural graphite powders. During this process, epoxy and hydroxyl groups lie on the surface of each graphene layer, while the carboxyl groups are located near the edges of basal planes of the graphite structure.[34,38] Simultaneously, carbon hydrolyzation occurred and the sp^2 bonds changed to sp^3 bonds. At the same time, NO_3^-, or SO_4^{2-} ions could insert themselves into the graphene layer, inducing an increase in the interlayer spacing.[39–41]

Initially, in order to examine the effect of oxidation time on preparation of graphene oxide and interlayer spacing, oxidation reactions with HNO_3/H_2SO_4 in 1:2 volume ratio and in during time 1 to 7 days were investigated. X-Ray diffraction patterns at various oxidation stages are shown in Fig. 1. As oxidation proceeds, the intensity of the (002) diffraction line (*d*-space 3.35 Å at 26.4°) in natural graphite was finally disappeared. Simultaneously, the GO exhibited only one peak at 12.2° (Fig. 1). Also, the X-ray diffraction pattern indicated that after 4 days of oxidation treatment, the graphite powders were completely oxidized to graphite oxide.

The interlayer distance between neighboring graphite oxide layers in GO was increased with oxidation for 4 days (they are ~ 7.22 Å apart), because of the intercalation using oxygen-containig groups and moisture. Increasing the reaction time (> 96 h) did not show any remarkable effect on the oxidation reaction and interlayer spacing (proved by the absence of further changes in the XRD analysis, Fig. 1).

In the second route: examination of the effect of HNO_3/H_2SO_4 amount on interlayer spacing and its comparison, oxidation of graphite with nitric acid and sulfuric acid in 1:3 volume ratio (modified *Staudenmaier* method) for 4-day was performed.Resulted in a slightly expanded interlayer distance to 9.13 Å ($2\theta = 11.6°$). Therefore, further increasing of oxidant agents in modified *Staudenmaier* method is more beneficial than *Staudenmaier* procedure. In general, well-oxidized carbon atoms results in an increase in the interlayer spacing of GO relative to natural graphite. Hence, the interlayer distances can be increased from 3.35 Å of the original graphite to 7.22 Å in *Staudenmaier* method and 9.13 Å in modified *Staudenmaier* method.

The FT-IR spectra of GO (a) in during time 4 days and (b) modified method are presented in Fig. 2, respectively. As it can be seen, the characteristic peaks of graphene oxide such as the stretching vibration of hydroxyl group (–OH), the stretching vibration of C=O from carboxylic group, the vibration of O=C–O from carboxylate and the vibration of C–O alcohol and C–O–C of epoxy groups centered at 3443, 1735, 1401, 1207 and 1055 cm^{-1}, respectively. Also, the peak at 1629 cm^{-1} is attributed to the vibrations of unoxidized graphitic domains, in these samples.[42] FT-IR spectra images of the two samples indicate that, peaks intense for GO in modified method is sharper than the same peak for GO 4 days and support the assertion that GO modified has a more oxidation than GO 4 days.

Raman spectroscopy is a powerful nondestructive tool to characterize carbon materials, particularly for distinguishing ordered and disordered crystal structures of carbon. The oxidation leads to a huge reduction in the size of graphite nanosheets in GO, compared to the size of the natural graphite flakes.[34] The Raman spectrum of the GO obtained using the modified Staudenmaier method displays a strong G line at 1592 cm^{-1} assigned to the E_{2g} phonon of carbon sp^2 atoms, while the D line at 1332 cm^{-1} attributed to a breathing mode of κ-point phonons of A_{1g} symmetry, which is attributed to local defects and disorders. The overtone of the D line is located at 2622 cm^{-1} (Fig. 3).

To identify the functional groups of GO obtained using the modified *Staudenmaier* method, XPS curve-fitted and survey C1s spectra of GO are presented in Fig. 4. The XPS spectrum of GO (Fig. 4a), clearly indicates a considerable degree of oxidation with five components that correspond to carbon atoms in different functional groups: the un-oxidized sp^2 carbons or C=C at 284.3 eV, the oxidized sp^3 carbons or C–C at 285.6 eV, the C–O bonds, which correspond to the epoxide and hydroxyl groups at 286.7 eV, the C=O from carboxylic group at 287.5 eV and O=C–O bond attributed to carboxylate group at 289.03 eV (Table 1). Moreover, in Fig. 4b two peaks centered at

286.8 eV and 533.9 eV can be assigned to C1s and O1s signals.[43,44] The peak O1s is higher than the peak C1s for GO. This result indicates that the full oxidation of graphite powders can be achieved. In addition, the relative atomic percentage of various functional groups in GO are given in Table 1.

Table 1. The C1s peak position and the relative atomic percentage of various functional groups in GO obtained using the modified *Staudenmaier*, graphene using different reducing agents and functionalized graphene with ODA.

Samples	Fitting of the C1s peak binding energy					
	C=C sp^2 (eV)(%)	C–C sp^3 (eV)(%)	C–O (eV)(%)	C=O (eV)(%)	O=C–O (eV)(%)	C–N (eV)(%)
GO	284.3 (6.1)	285.6 (39.7)	286.7 (13.4)	287.5 (31.4)	289.03 (2.9)	–
G-Hydroquinone	284.7 (16.8)	285.6 (50.1)	286.7 (18.2)	287.5 (7.2)	288.3 (7.8)	–
G-Hydrazine hydrate	284.8 (27.9)	285.6 (29.2)	286.7 (14.2)	287.5 (7.7)	288.4 (3.2)	–
G-ODA	284.3 (1.8)	285.6 (33.3)	286.7 (20.5)	287.5 (23.5)	289.03 (9.0)	285.9 (10.5)

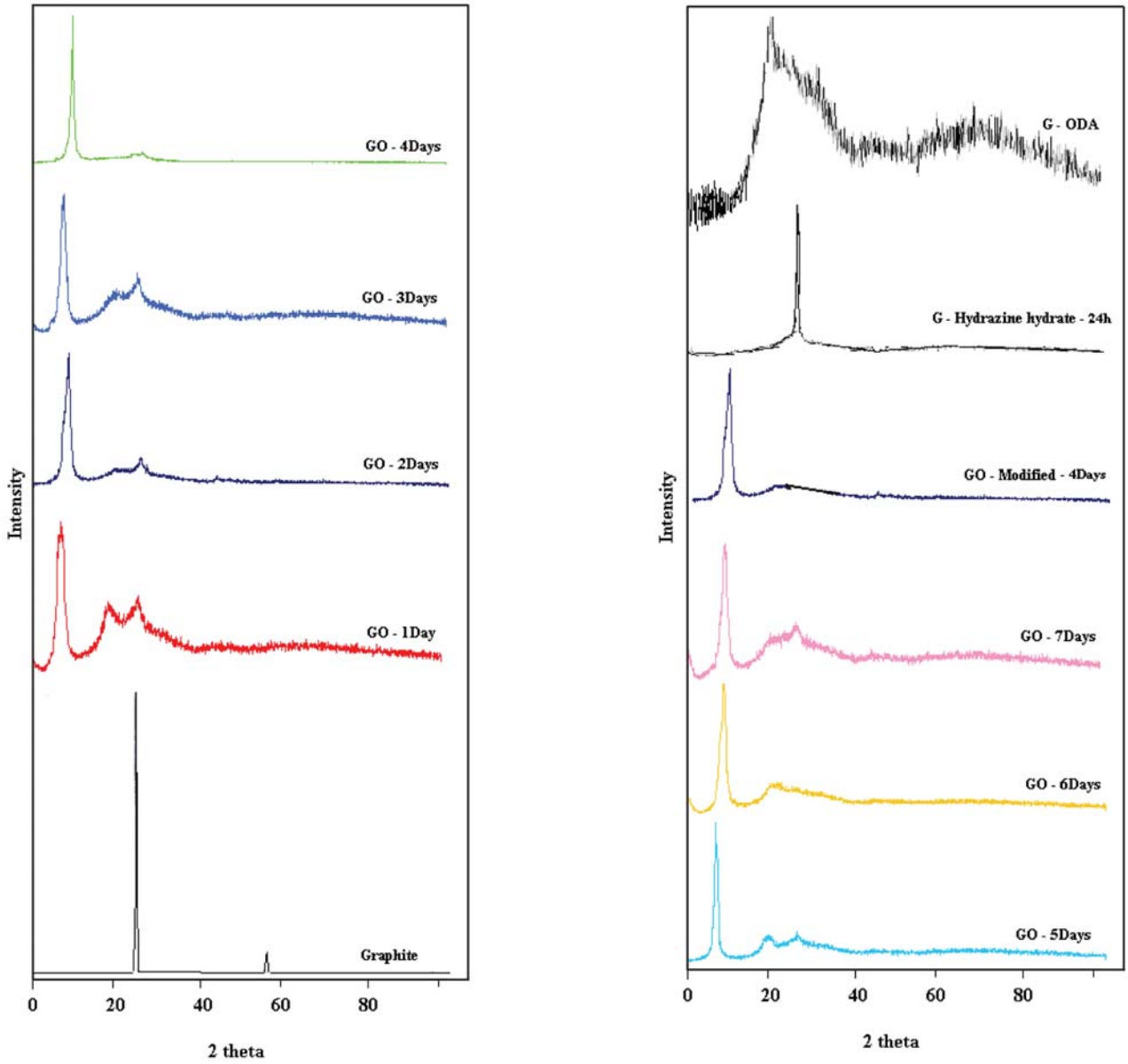

Fig. 1. X-ray diffraction patterns of graphite, graphene oxide obtained using *Staudenmaier* method (HNO_3/H_2SO_4 in 1:2 volume ratio) at 1–7 days, graphene oxide obtained using modified *Staudenmaier* method (HNO_3/H_2SO_4 in 1:3 volume ratio) at 4 days, graphene and functionalized graphene.

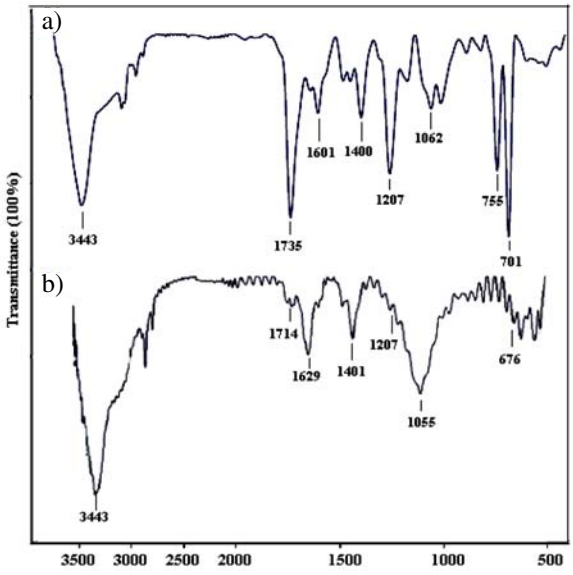

Fig. 2. FT-IR spectra of graphene oxide (a) Staudenmaier and (b) modified method.

Figure 5 shows the SEM micrographs of GO. The appearance of bright edges and smooth stages across the area arises from the presence of oxygenated functional groups. Also, its layers are transparent and very thin.

Numerical and visual characterizations play an important role in the overall interpretation of surface topography. In fact, it is stated clearly that the 3D characteriza-

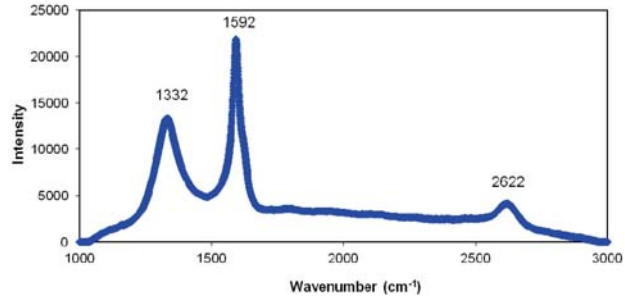

Fig. 3. Raman spectrum of graphene oxide nanosheets.

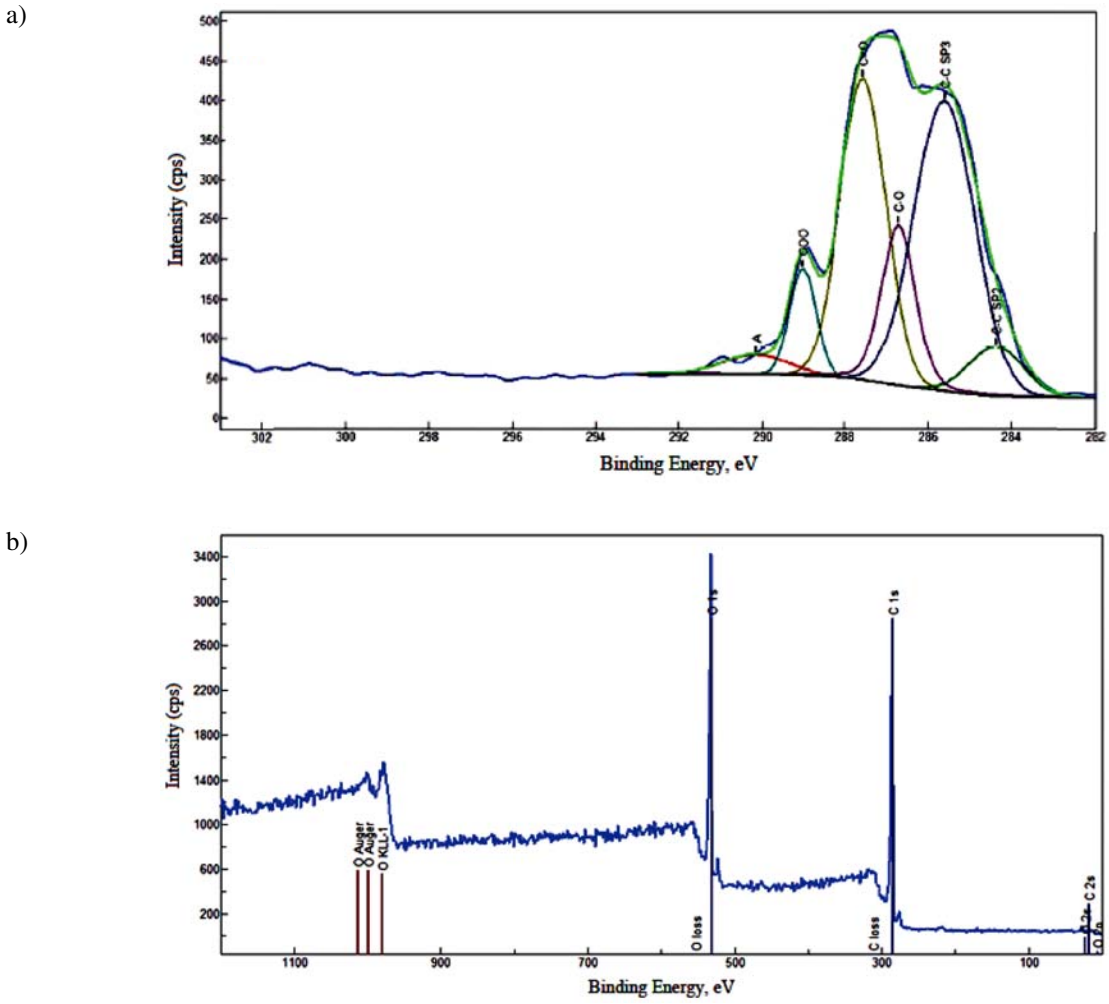

Fig. 4. XPS (a) curve-fitted and (b) survey C1s spectra of graphene oxide nanosheets obtained using the modified *Staudenmaier* method.

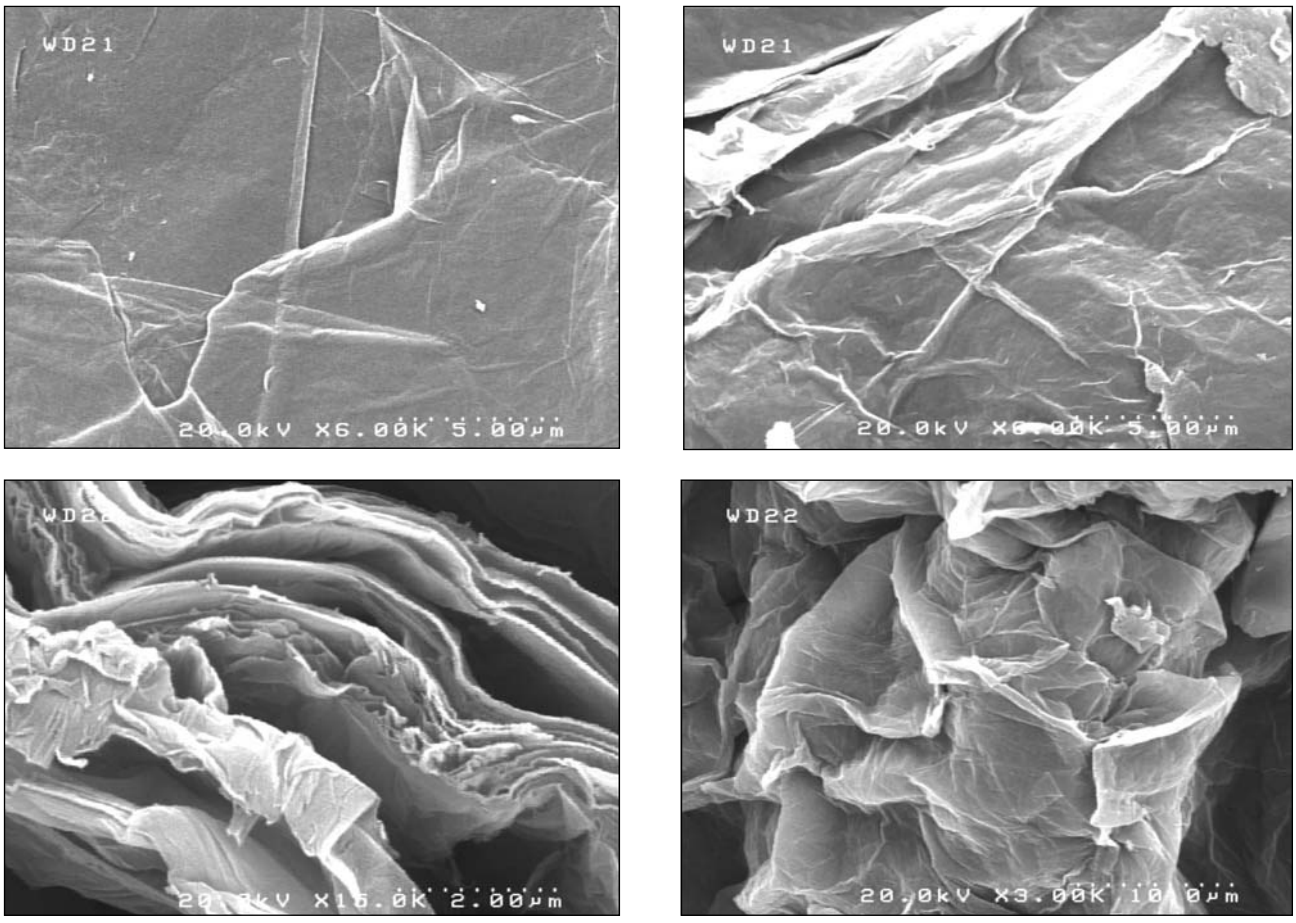

Fig. 5. SEM images of graphene oxide nanosheets.

tion of surface topography must include both numerical and visual characterization. The recorded data can be presented in different ways: as profile peaks, surface valley depth, height distribution columns etc. Two parameters (i.e., the profile scan and height distribution) were used in this investigation. The results of surface topography measurements are presented in Fig. 6. The exfoliation to achieve graphene oxide sheets obtained using the modified *Staudenmaier* method has been most typically confirmed by thickness measurements of the single graphene sheet (~1.1 nm height) using atomic force microscopy.

3. 2. Characterization of Graphene Nanosheets

After chemical reduction through refluxing with hydroquinone and hydrazine hydrate, graphene oxide nanosheets were reduced to graphene nanosheets and restored to an ordered crystal structure.

Figure 7 shows the XRD patterns of GO before and after treatment with hydroquinone and hydrazine hydrate as reducing agents in the different times. We observe gradual changes in the patterns after 22 and 24h reaction time for reduction with hydroquinone and hydrazine hydrate. The interlayer distance obtained using the modified *Staudenmaier* method is 9.13 Å (2θ = 12.2°) with reduction, the interlayer distance is expected to contract due to the removal of such functional groups. The peak of the large interlayer distance disappeared completely and a peak near 3.356 and 3.361Å (2θ = 26.5°) respectively for hydrazine hydrate and hydroquinone became visible. This implied that most of the functional groups were removed after the reduction.

Raman spectroscopy was employed to analyze the structural changes during chemical processing from graphene oxide to reduced graphene oxide. After chemical reduction of graphene oxide, the conjugated graphene network (sp^2 carbon) will be reestablished. However, the size of the reestablished graphene network is usually smaller than the original graphite layer, which will lead to the increase of intensity of the D/G consequently. As seen from Fig. 8, the Raman spectrum of reduced graphene oxide obtained using hydroquinone and hydrazine hydrate as reducing agents contains both G band which shifted back to 1584 cm^{-1} and D band at 1312 cm^{-1}.

The XPS curve-fitted and survey C1s spectra of reduced graphene oxide with hydrazine hydrate in during 24 h are presented in Fig. 9. The reduction process elimina-

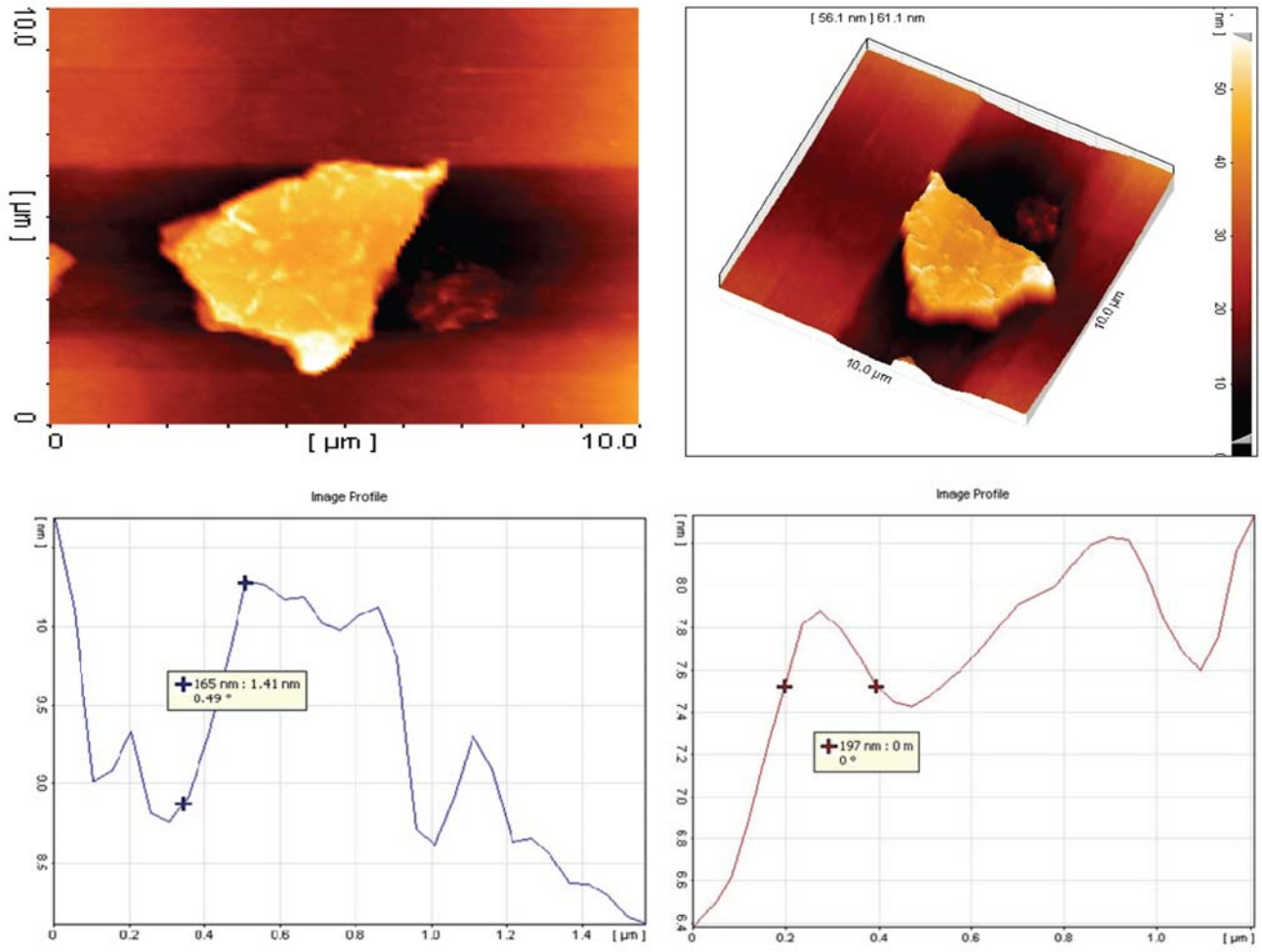

Fig. 6. AFM images of graphene oxide nanosheets.

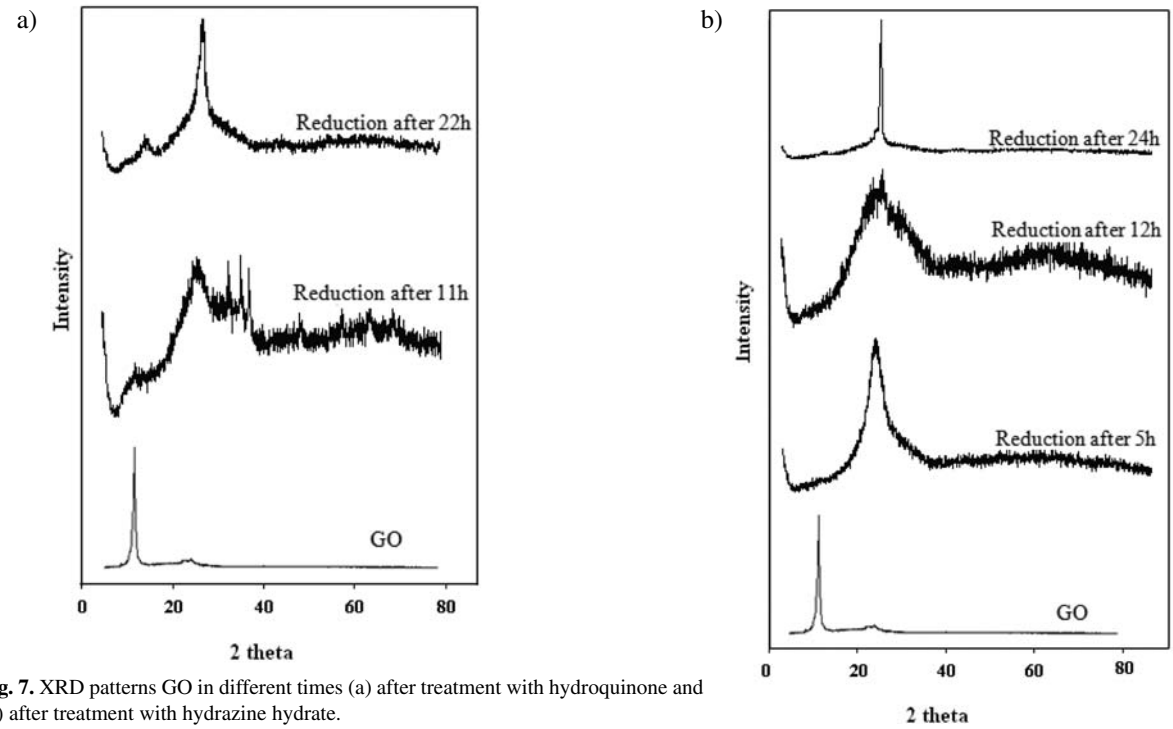

Fig. 7. XRD patterns GO in different times (a) after treatment with hydroquinone and (b) after treatment with hydrazine hydrate.

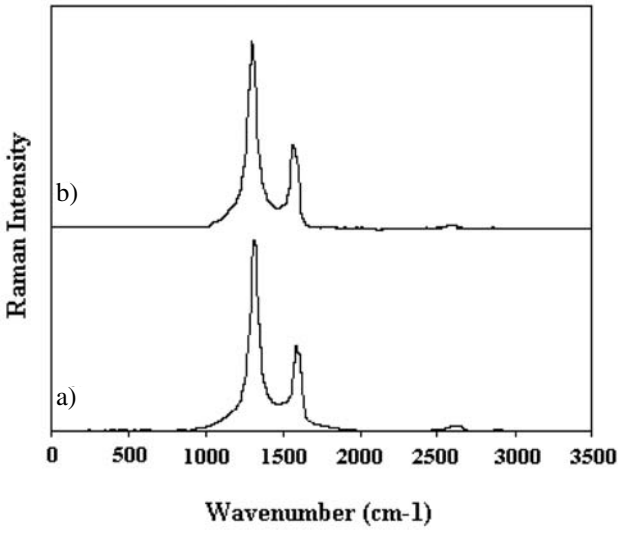

Fig. 8. Raman spectrum of graphene nanosheets obtained using (a) hydroquinone and (b) hydrazine hydrate.

ted much of the oxygen on the surface of GO, resulting in the restoration of the conjugated graphene network. Seen from Table 1, the C=O bonds decreased significantly in all samples, which was probably due to the reduction of carboxylic groups. Meanwhile, in Fig. 9b two peaks centered at 286.8 eV and 533.9 eV can be assigned to C1s and O1s signals. The peak C1s is higher than the peak O1s for graphene nanosheets. This indicates that the restoration a part of conjugated graphene networks can be achieved by the increase in sp^2 carbon content.

Figure 10 illustrates the SEM images of graphene. The view of reduced graphene oxide reveals the agglomeration of rippled silk-like graphene. Also, images of graphene further confirm the appearance of transparent with wrinkles and folds.

Hydrazine hydrate, unlike other strong reductants, does not react with water and was found to be the best one in producing very thin and fine graphite-like sheets.[45,46] Also, the other advantages of this reductant agent are simpler protocol and higher yield.

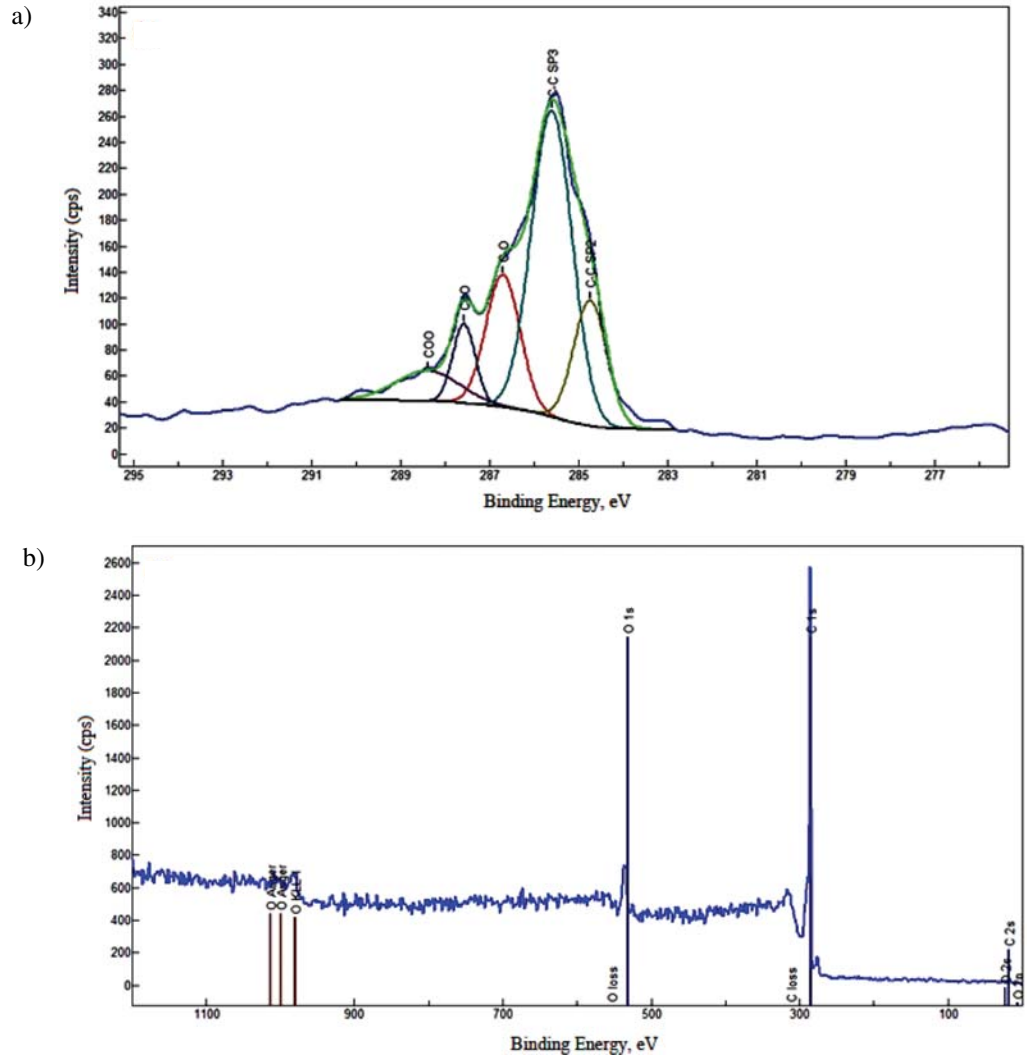

Fig. 9. XPS (a) curve-fitted and (b) survey C1s spectra of graphene nanosheets.

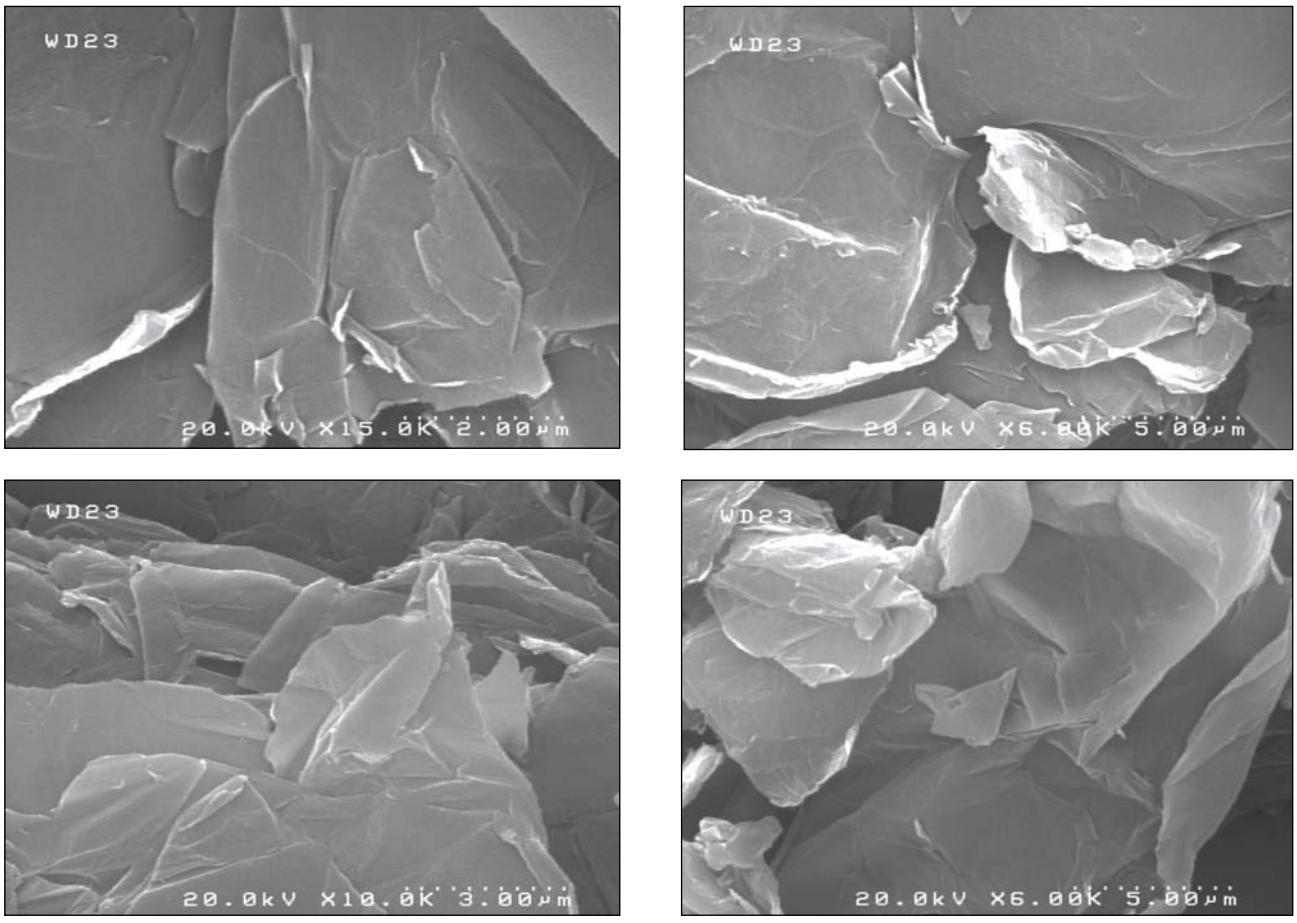

Fig. 10. SEM images of graphene nanosheets.

3. 3. Characterization of Functionalized Graphene Nanosheets

Graphene nanosheets that are freshly prepared *via* chemical reduction are non-dispersible in solvent. We prepared soluble graphene nanosheets by attaching octadecylamine (ODA) molecules to the graphene oxide obtained using the modified *Staudenmaier* method and reduction by hydroquinone through a reflux process. In the first step, GO nanosheets react with ODA and form GO-ODA, during which the carboxyl groups react with the amine in ODA by the formation of the amide bond. In the second step, GO-ODA nanosheets were reduced to G-ODA by hydroquinone (Scheme 1).

Figure 11 shows FT-IR spectra (a) graphene obtained using hydroquinone and (b) functionalized graphene with ODA. The intense asymmetric bands of the alkyl

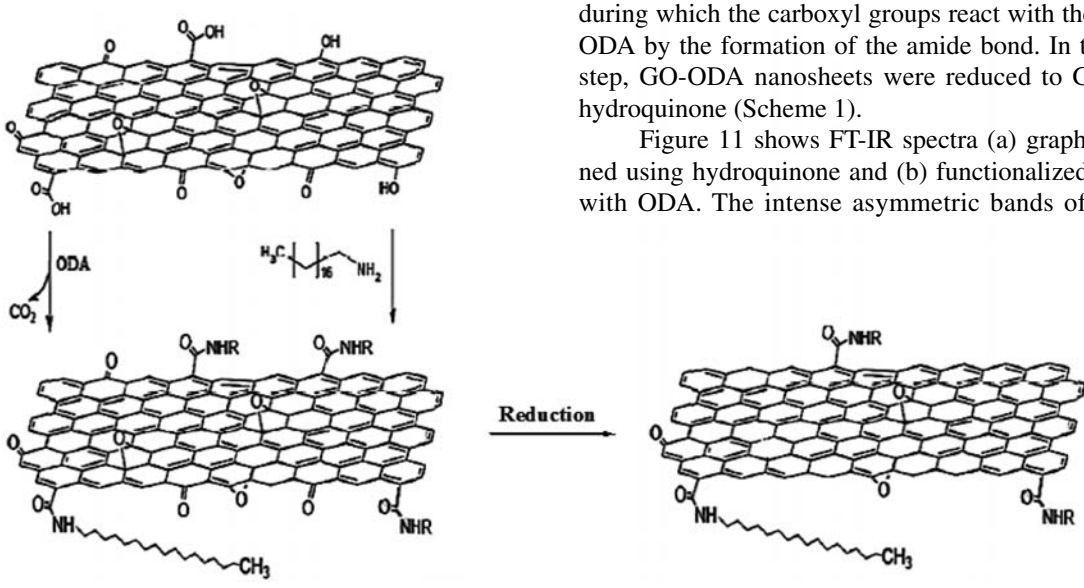

Scheme 1. The synthesis route of functionalized graphene with ODA.

group at 2848 and 2919 cm^{-1} correspond to the C–H stretching vibrations in ODA. We also observed a band indicating the amine group (N–H) at 1459 cm^{-1} for ODA attached to graphene.[37]

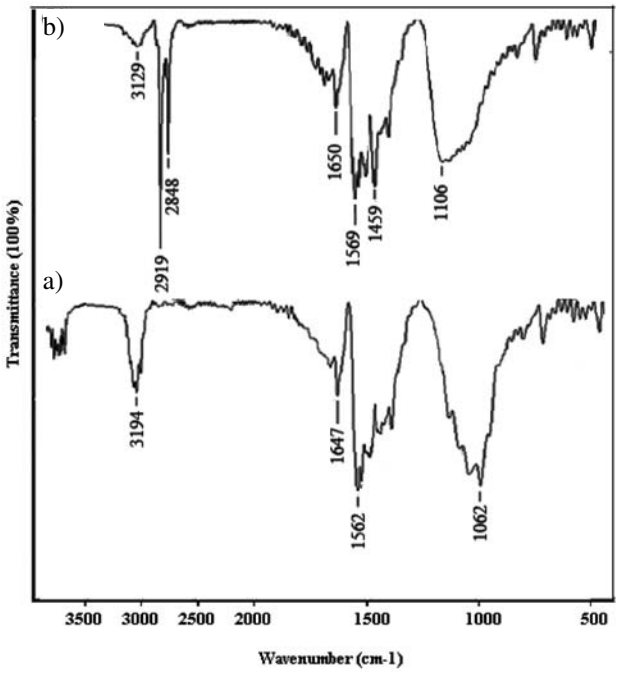

Fig. 11. FT-IR spectra of (a) graphene nanosheets obtained using hydroquinone and (b) functionalized graphene with ODA.

Figure 12 depicts the XRD patterns of graphene nanosheets obtained from hydroquinone and (b) functionalized graphene with ODA. The graphene nanosheets show a peak at (2θ = 26.5°) with interlayer distance 3.361 Å, which is almost the same as that of graphite. For functionalized graphene, the strongest diffraction peak appearing at (2θ = 22.1°) correspond to a *d*-spacing of 4.01Å, which is slightly higher than that of the graphene nanosheets. Interlayer spacing between graphene sheets increases due to functionalization of graphene sheets by ODA molecules.

Raman spectra of (a) graphene obtained using hydroquinone as reducing agent and (b) functionalized graphene with ODA are shown in Fig. 13. After chemical modification of graphene, the Raman spectrum of G-ODA contains both G band at 1578 cm^{-1} and D band at 1309 cm^{-1}. The results from the XRD and Raman spectra imply that the structure of the graphene nanosheets has been maintained after chemical functionalization.

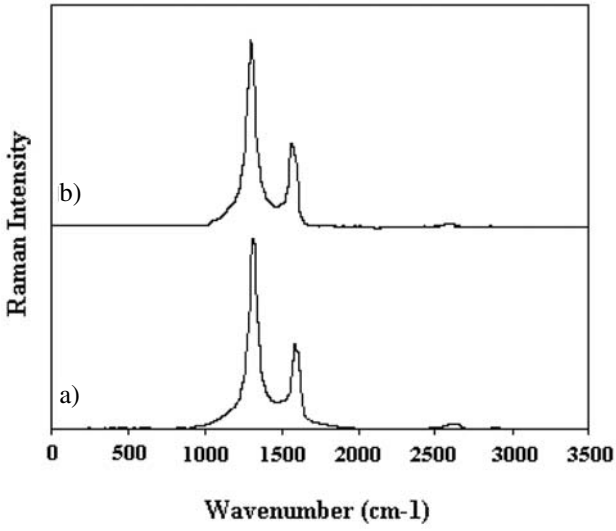

Fig. 13. Raman spectrum of (a) graphene nanosheets obtained using hydroquinone and (b) graphene functionalized with ODA.

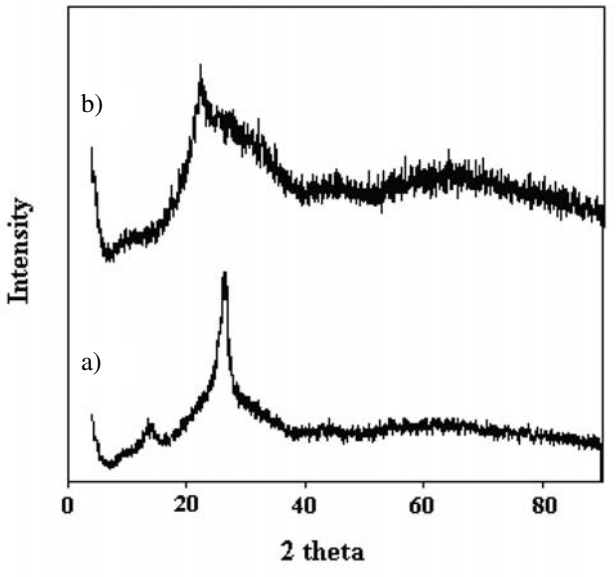

Fig. 12. X-ray diffraction patterns of (a) graphene nanosheets obtained using hydroquinone and (b) functionalized graphene with ODA.

We have employed XPS for the surface information of G-ODA. To identify the functional groups, both the XPS curve-fitted and survey C1s spectra of G-ODA are presented in Fig. 14. The XPS spectrum of G-ODA, clearly indicates a considerable degree of functionalization of surface graphene with six components that correspond to carbon atoms in different functional groups: the non-oxygenated carbons or C=C sp^2 at 284.3 eV, the sp^3 carbons or C–C at 285.6 eV, the C–N bonds, which correspond to ODA molecules attached to the graphene nanosheets at 285.9 eV, the C–O bonds, which correspond to the epoxide and hydroxyl groups at 286.7 eV, the C=O from amide group at 287.5 eV and O=C–O bond attributed to carboxylate group at 289.03 eV (Fig. 14 a). As shown in Fig. 14b, there are three elements in the XPS spectra, namely carbon, nitrogen and oxygen without other elements. The peaks centered at 286.8 eV, 399.8 eV and 533.9 eV can be assigned to C1s, N1s and O1s signals. Also, the relative

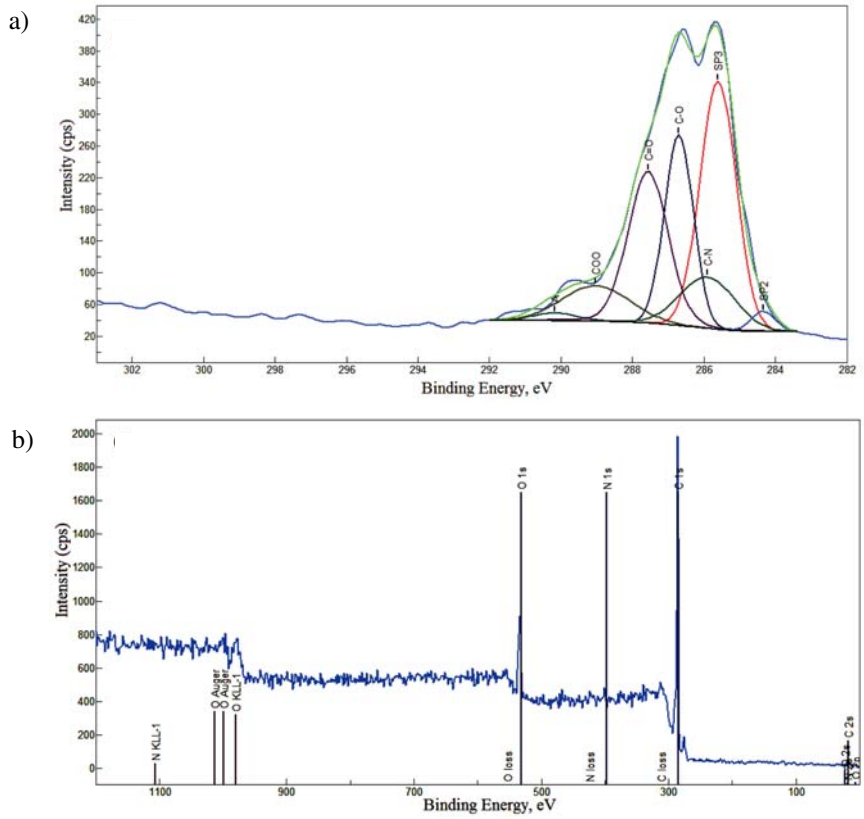

Fig. 14. XPS (a) curve-fitted and (b) survey C1s spectra of graphene nanosheets functionalized with ODA.

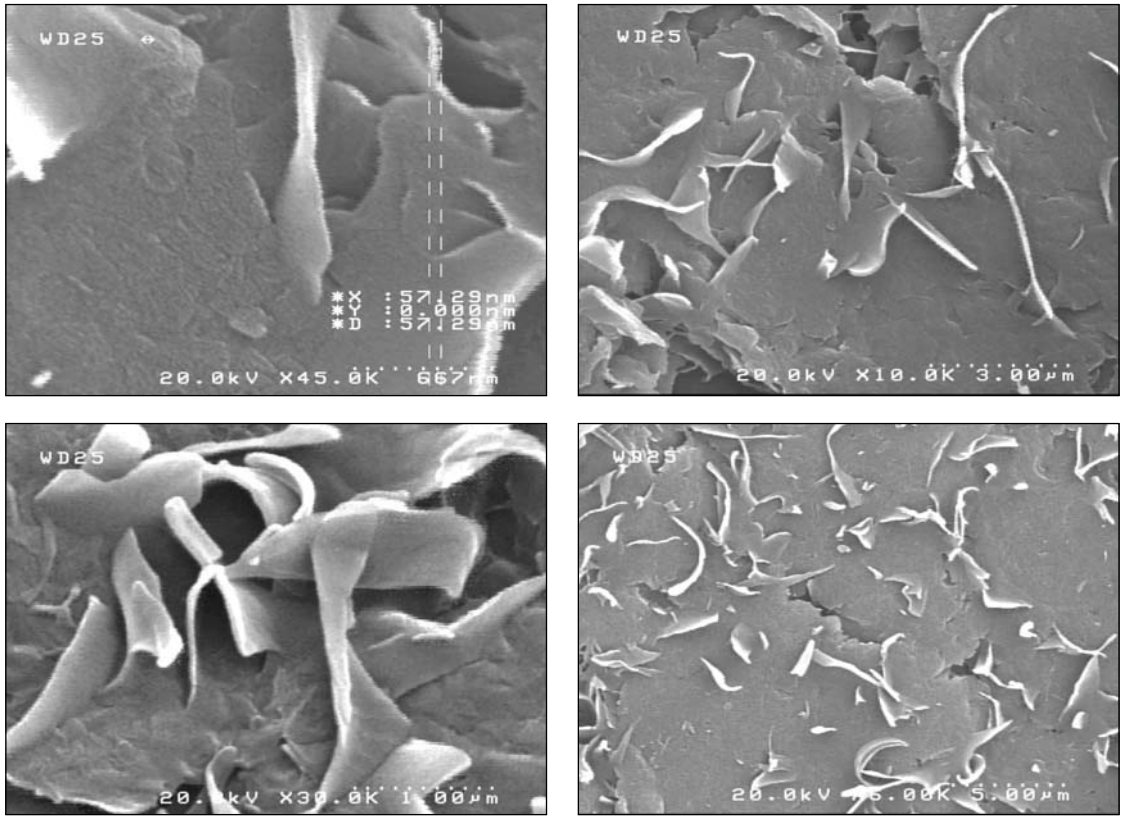

Fig. 15. SEM images of graphene functionalized with ODA.

atomic percentage of various functional groups is given in Table 1.

Scanning electron microscopy images of G-ODA nanosheets are shown in Fig. 15. Transparent and resembling rippled silk waves, are clearly observed.

4. Conclusions

The modified *Staudenmaier* method *via* performing oxidation reaction of graphite with HNO_3/H_2SO_4 in 1:3 volume ratio at 4 days, improved the efficiency of the oxidation process of *Staudenmaier* for the preparation of graphene oxide. It is to be noted that all the experiments such as reduction and fictionalization, the initial oxide was used based on the modified *Staudenmaier* method with high exfoliation degree. The chemical reduction of graphene oxide was studied using the common reducing agents such as hydroquinone and hydrazine hydrate. The advantages of hydrazine hydrate are simpler protocol and higher yield. Therefore, treatment of graphene oxide with hydrazine hydrate can be better than hydroquinone. After surface fictionalization, the crystal structure of the graphene nanosheets was maintained intact.

5. References

1. K. S. Novoselov, A. K. Geim, S. V. Morozov, D. Jiang, Y. Zhang, S. V. Dubonos, I. V. Griogrieva, A. A. Firsov, *Science*, **2004**, *306*, 666–669.
2. M. S. Dresselhaus, G. Dresselhaus, *Advances in Physics*, **2002**, *51*, 1–186.
3. Y. Zhang, Y.-W. Tan, H. L. Stormer, P. Kim, *Nature*, **2005**, *438*, 201–204.
4. Y. Zhang, J. P. Small, M. E. S. Amori, P. Kim, , **2005**, *94*, 176803.
5. C. Berger, Z. M. Song, X. B. Li, X. S. Wu, N. Brown, C. Nand, D. Mayon, T. B. Li, J. Hass, A. N. Marchenkov, E. H. Conrad, P. N. First, W. A.de Heer, *Science*, **2006**, *312*, 1191–1196.
6. C. Berger, Z. M. Song, T. B. Li, X. B. Li, A. Y. Ogbazghi, R. Feng, Z. T. Dai, A. N. Marchenkov, E. H. Conrad, P. N. First, W. A.de Heer, **2004**, *108*, 19912–19916.
7. K. S. Novoselov, A. K. Geim, S. V. Morozov, D. Jiang, M. I. Katsnelson, I. V. Grigorieva, S. V. Dubonos, A. A. Firsov, *Nature*, **2005**, *438*, 197–200.
8. S. Wang, P. J. Chia, L. L. Chua, L. H. Zhao, R. G. S. Goh, *Adv. Mater.*, **2008**, *20*, 3440–3446.
9. S. Niyogi, A. Hamon, H. Hu, B. Zhao, P. Bhowmik, R. Sen, M. E. Itkis, *Acc. Chem. Res.*, **2002**, *35*, 1105–1113.
10. Y. Hernandez, V. Nicolosi, M. Lotya, F. M. Blighe, Z. Sun, S. De, I. T. McGovern, B. Holland, M. Byrne, Y. K. Gun'ko, J. J. Boland, P. Niraj, G. Duesberg, S. Krishnamurthy, R. Goodhue, J. Hutchison, V. Scardaci, A. C. Ferrari, J. N. Coleman, *J. Nature Nanotechnol.*, **2008**, *3(9)*, 563–568.
11. B. Lamg, *Surface Sci.*, **1975**, *53*, 317–329.
12. E. Rokuta, Y. Hasegawa, A. Itoh, K. Yamashita, T. Tanaka, S. Otani, C. Oshima, *Surface Sci.*, **1999**, *427*, 97–101.
13. H. Shioyama, *J. Mate. Sci. Lett.*, **2001**, *20*, 499–500.
14. K. S. Novoselov, D. Jiang, F. Schedin, T. J. Booth, V. V. Khotkevich, S. V. Morozov, A. K. Geim, *PNAS.*, **2005**, *102*, 10451–10453.
15. P. R. Somani, S. P. Somani, M. Umeno, *Chemical Physics Lett.*, **2006**, *430*, 56.
16. J. J. Wang, M. Y. Zhu, R. A. Outlaw, X. Zhao, D. M. Manos, B. C. Holoway, *Appl. Phys. Lett.*, **2004**, *85*, 1265.
17. J. J. Wang, M. Y. Zhu, R. A. Outlaw, X. Zhao, D. M. Manos, B. C. Holoway, *Carbon*, **2004**, *42*, 2867.
18. S. Stankovich, D. A. Dikin, G. H. B. Dommett, K. M. Kohlhaas, E. J. Zimney, E. A. Stach, R. D. Piner, S. T. Nguyen, R. S. Ruoff, *Nature*, **2006**, *442*, 282.
19. R. Verdejo, F. Barroso-Bujans, M. A. Rodriguez-Perez, J. A. de Saja, M. A. Lopez-Manchado, *J.Mat. Chem.*, **2008**, *18*, 2221.
20. H. C. Schniepp, J. L. Li, M. J. McAllister, H. Sai, M. Herrera Alonso, D. H. Adamson, R. K. Prud'homme, R. Car, D. A. Saville, I. A. Aksay, *J. Phys. Chem. B*, **2006**,*110*, 8535.
21. S. Gilje, S. Han, M. Wang, K. L. Wang, R. B. Kaner, *Nano Lett.*, **2007**, *7*, 3394.
22. C. Gomez Navarro, R. T. Weitz, A. M. Bittner, M. Scolari, A. Mews, M. Burghard, K. Kern, *Nano Lett.*, **2007**, *7*, 3499.
23. D. A. Dikin, S. Stankovich, E. J. Zimney, R. D. Piner, G. H. B. Dommett, G. Evmenenko, *Nature*, **2007**, *448*, 457–460.
24. M. Hirata, T. Gotou, S. Horiuchi, M. Fujiwara, M. Ohba, *Carbon*, **2004**, *42*, 2929–2937.
25. Z. S. Wu, W. Ren, L. Gao, B. Liu, C. Jiang, H. M. Cheng, *Carbon*, **2009**, *47*, 493–499.
26. S. Lee, S. Lim, E. Lim, K. Lee, *Journal of Physics and Chemistry of Solids*, **2010**, *71*, 483–486.
27. W. Choi, I. Lahiri, R. Seelaboyina, Y. S. Kang, *Critical Reviews in Solid State and Materials Sciences*, **2010**, *35*, 52–71.
28. J. Shen, Y. Hu, M. Shi, X. Lu, C. Qin, C. Li, M. Ye, *Chem. Mater.*, **2009**, *21*, 3514–3520.
29. S. Horiuchi, T. Gotou, M. Fujiwara, T. Asaka, T. Yokosawa, Y. Matsui, *Appl. Phys. Lett.*, **2004**, *84*, 2403–2405.
30. B. C. Brodie, *Proc. R. Soc. Lond.*, **1859**, *10*, 249–259.
31. W. S Jr Hummers, R. E. Offeman, *J. Am. Chem. Soc.*, **1958**, *80*, 1339.
32. D. C. Marcano, D. V. Kosynkin, J. M. Berlin, A. Sinitskii, Z. Sun, A. Slesarev, L. B. Alemany, W. Lu, J. M. Tour, *ACS Nano* **2010**, *4*, 4806–4814.
33. L. Staudenmaier, *Ber. Dtsch. Chem. Ges.*, **1898**, *31*, 1481–1487.
34. S. Stankovich, D. A. Dikin, R. D. Piner, K. A. Kohlhaas, A. Lleinhammes, Y. Jia, Y. Wu, *Carbon*, **2007**, *45*, 1558–1565.
35. Y. Geng, S. J. Wang, J-K Kim, *J. Colloid and Interface Science* **2009**, *336*, 592–598.
36. A. B. Bourlinos, D. Gournis, D. Petridis, T. Szabo, A. Szeri, I. Dekany, *Langmuir*, **2003**, *19*, 6050–6055.
37. G. Wang, X. Shen, B. Wang, J. Yao, J. Park, *Carbon*, **2009**, *47*, 1359–1364.

38. N. I. Kovtyukhova, P. I. Olliver, B. R. Martin, E. V. Buzaneva, *Chem. Mat.*, **1999**, *11*, 771–778.
39. C. Hontoria-Lucas, A. López-Peinado, J. López-González, R. Martin-Aranda, *Carbon*, **1995**, *33*, 1585–1592.
40. H. He, J. Klinowski, M. A. Foster, A. Lerf, *Chem. Phys. Lett.*, **1998**, *287*, 53–56.
41. H. He, T. Riedl, A. Lerf , J. Klinowski, *J. Phys. Chem.*, **1996**, *100*, 19954–19958.
42. Y. X. Xu, H. Bai, G. W. Lu, C. Li, *J. Am. Chem. Soc*., **2008**, *130*, 5856–5857.
43. Y. Geng, S. J. Wang, J-K Kim, *J. Colloid and Interface Science* **2009**, *336*, 592–598.
44. T. I. T. Okpalugo, P. Papakonstantinou, H. Murphy, J. McLaughlin, N. M. D. Brown, *Carbon* **2005**, *43*, 153–161.
45. S. Stankovich, R. D. Piner, X. Q. Chen, N. Q. Wu, S. T. Nguyen, R. S. Ruoff, *J. Materials Chemistry*, **2006**, *16*, 155.
46. V. Singh, D. Joung, L. Zhai, S. Das, S. I. Khondaker, S. Seal, *Progress in Materials Science*, **2011**, *56*, 1178–1271.

Povzetek

V članku je predstavljena primerna kemijska metoda priprave nanoplastigrafenovega oksida. Z namenom preučevanja vpliva razmerij HNO_3/H_2SO_4 na medmrežne razdalje smo oksidirali grafit sHNO_3 in H_2SO_4 v volumskih razmerjih 1:2 in 1:3. Optimalne rezultate smo dosegli, če je reakcija potekala štiri dni in v primeru, ko je bilo volumsko razmerje med HNO_3 in H_2SO_4 enako 1:3 (uporabljena je bila modificirana metoda po Staudenmaierju). Glede na rezultate lahko rečemo, da modificirana metoda po Staudenmaierju izboljša učinkovitost tvorbe plasti in oksidacijski proces. Preučevali smo tudi kemijsko redukcijo grafenovega oksida s hidrokinonom in hidrazinovim hidratom. Na osnovi rezultatov lahko sklepamo, da je hidrazinov hidrat kot reducirni reagent primernejši od hidrokinona. Opisana je tudi priprava grafenskih-nanoplasti, površinsko funkcionaliziranih z oktadecilaminom. Produkte smo karakterizirali z različnimi instrumentalnimi tehnikami: infrardečo spektroskopijo (FT-IR),ramansko spektroskopijo, rentgensko praškovno difrakcijo(XRD), mikroskopijo na atomsko silo (AFM), vrstično elektronsko mikroskopijo na poljsko emisijo (FE-SEM), rentgensko fotoelektronsko spektroskopijo (XPS).